Available online at www.sciencedirect.com

jmr&t Journal of Materials Research and Technology

journal homepage: www.elsevier.com/locate/jmrt

Original Article

Development of Ti–In alloys by powder metallurgy for application as dental biomaterial

L. Romero-Resendiz [a,*,1], P. Gómez-Sáez [b,1], A. Vicente-Escuder [b], V. Amigó-Borrás [b]

[a] Instituto de Investigaciones en Materiales, Universidad Nacional Autónoma de México, Circuito Exterior S/N, Cd. Universitaria, A. P. 70-360, Coyoacán, CP, 04510, Mexico

[b] Universitat Politècnica de València, Instituto de Tecnología de Materiales, Camino de Vera S/N, 46022 Valencia, Spain

ARTICLE INFO

Article history:
Received 15 October 2020
Accepted 4 February 2021
Available online 13 February 2021

Keywords:
Ti–In alloys
Biomaterial
Powder metallurgy
Ion release
Electrochemical behavior

ABSTRACT

Substantial progress has been made in Ti alloys' properties and chemical composition. However, the effect of porosity and indium content on biocompatibility and corrosion behavior has not been sufficiently studied. Indium (In) is a promising nontoxic element that can replace other toxic elements, while porosity is associated with a good biological response. The purpose of this paper is to evaluate the achievability of three Ti–In alloys with 2.5, 5, and 10 wt.% Indium by powder metallurgy methods as dental prostheses. The findings of the present work showed that In acted as a grain refiner, and allowed us to obtain an 11.2-fold reduction for the Ti–10In sample than for the Ti–2.5In alloy. The total porosity of the Ti–In alloys decreased according to In content, however, grain size and In content showed a greater effect on the mechanical behavior in comparison with the effect of porosity, probably because of the low porosity percentage. All the mechanical values fell within the ranges accepted in the literature for dental implant applications. The Ti^{3+} and In^{3+} ion releases were below the toxic concentrations for the human body, with a maximum of 0.43 and 0.016 $\mu g\ cm^{-2}\ h^{-1}$, respectively. Corrosion sensitivity decreased with In addition due to its surface protective effect on the Ti-matrix. These results proved that utilizing powder metallurgy methods, Ti–In alloys are feasible candidates for dental prosthesis. Of the three prepared Ti–In alloys, the Ti–10In alloy properties made it the most appropriate Ti–In alloy to be used as a dental implant.

* Corresponding author.
E-mail address: liliana.rom7@comunidad.unam.mx (L. Romero-Resendiz).
[1] L. Romero-Resendiz and P. Gómez-Sáez contributed equally to this work.

https://doi.org/10.1016/j.jmrt.2021.02.014

1. Introduction

Based on high dental prosthesis demands, research into new or enhanced alloys to obtain processes for biomaterials is decidedly relevant. Statistically speaking, "69% of adults ages 35 to 44 have lost at least one permanent tooth" due to accidents or oral diseases [1]. It is also estimated that "3 million people in the United States have dental implants", which implies continuously increasing demand [2]. For the above reasons, the development of new biomaterials, and the improvement of processing methodologies, are essentially relevant to advance in dentistry applications.

Dental materials must be able to interact with not only the stresses generated by chewing, but also with the different chemical substances present in the mouth and those that come from food, and all this with no inimical biological response for long periods. Such a biological response of materials depends on mechanico-physical properties, mainly corrosion susceptibility and ions released into the oral environment [3].

The use of titanium-based (Ti alloys) alloys for dental implants is widespread given their physical, mechanical, and biological properties [4–7], such as the good strength, stiffness, and ductility, as well as their low weight, high corrosion resistance, successful osseointegration, chemical stability, and non-ferromagnetic nature. Ti alloys report worthy advantages compared to the employment of commercially pure Ti (CP–Ti) for dental implants. The most important of these advantages is improved mechanical properties [8], lowering the high melting point of CP-Ti as a result of the alloy's elements, and better control of the high chemical reactivity of powder Ti compared to the liquid phase [9,10].

Likewise, the use of indium (In) as an alloying element in biomaterials may provide favorable performance. It has been reported that In can promote the formation of oxides, which are of utmost importance for bond strength at ceramic-metal interfaces [11]. There are also reports that introducing In into Ti-alloys can improve the necessary mechanical properties for dental implants, thus reducing the elastic modulus and allow it to come closer to that of bone [12]. In addition, In contents can improve physical properties, specifically corrosion resistance [8]. It is also worth mentioning that In is mentioned as a nontoxic element in materials for dental applications [8,13]. Moreover, the use of alpha-type Ti–In alloys normally focuses on applications in which corrosion resistance is a priority factor [14]. The In range herein used (2.5–10 wt.%) resulted in a single-hexagonal-alpha phase microstructure.

The development of porous materials for dental purposes has led to promising results. Apart from the general qualities that dentistry materials must meet, materials designed for dental implants must allow successful osseointegration [3]. The metallic materials developed by powder metallurgy for dental applications are extremely interesting for various scientific groups because the resulting porosity allows better anchorage to the organic tissue of bone [15–18], which can promote more efficient bonding [10]. Apart from all these virtues, a porous structure also enables body fluid transference by facilitating tissue generation [19].

Previous reports indicate that employing casting Ti–In binary alloys can be promising in the dental implants field due to increased mechanical strength and hardness, comparable cytotoxicity behavior [20] as well as similar corrosion resistance *versus* CP–Ti [21]. However, there are still many unknowns to be solved in Ti–In alloys, such as the role of porosity in biocompatibility, corrosion resistance, and mechanical performance. Developing Ti–In alloys by means of powder metallurgy methods makes them promising materials for use in oral implant applications and may have a strong impact on the dental industry.

The aim of this work is to determine the feasibility of porous Ti–In alloys produced by powder metallurgy process as dental implants. Three In contents were used in this study; i.e. 2.5, 5, and 10 wt.%. Electron microscopy and X-ray diffraction (XRD) analyses; bending and hardness tests; ion release and corrosion measurements were carried out to evaluate the microstructural, mechanical, and physical behaviors of alloys, respectively.

2. Experimental procedure

2.1. *Sintering process of Ti–In alloys*

Commercially available Ti and In powders (99.7% purity) from the Atlantic Equipment Engineers and Alfa Aesar companies, respectively, were used as the raw material to produce Ti–In binary alloys. The average particle size for Ti as received was 44 μm, with 25–30 μm for In. Elemental powder mixtures were prepared for three different weight ratios: Ti–2.5In, Ti–5In, and Ti–10In. Five samples were obtained for each composition ratio. The mixing process was performed in a BioEngineering powder mixer model Inversina at 45 rpm for 45 min in an argon atmosphere. Stainless steel balls (5 mm radius) were used to avoid dust agglomeration during mixing. Green samples (30 × 12 × 5 mm) were obtained by cold isostatic pressing at 600 MPa with an Instron hydraulic press model 1343. A five-step sintering process was carried out in a Carbolite HVT 15/75/450 tubular furnace at 10^{-2} Pa vacuum. The five sintering steps were: 1) heating at 10 °C/min to a temperature close to the allotropic Ti change; 2) keeping the temperature at 825 °C for 3 h; 3) a heating rate of 7 °C/min up to 1300 °C; 4) maintaining temperature for 3 h; 5) furnace cooling until room temperature. A monophasic alpha-Ti microstructure is expected within the In range (2.5–10% by weight) used in this work [22], being the reason for carrying out the sintering process of the three alloys at the same temperatures. It is worth mentioning that the inclusion of the second step ensured homogeneity during the Ti phase transformation, and allowed In to solubilize, which decreases its sublimation.

2.2. *Microstructural evaluation*

Before the microstructural examination, samples were subjected to conventional metallographic preparation with SiC grinding paper with progressive grit size from 220 to 1200. Polishing was carried out until a mirror finishing appearance with a 9 μm diamond suspension and then colloidal silica suspension of 0.05 μm in particle size. The specimens used for

optical microscopy (OM) were etched with Kroll's reagent (10 mL HF + 50 mL HNO_3 + 100 mL H_2O). An ultrasonic bath was used for 20 min to clean samples. The morphological and microstructural observations were recorded by using OM (Nikon LV100) and scanning electron microscopy (SEM-Zeiss Auriga Compact model). The present phases were characterized using a Bruker X-ray diffractometer D2 Phaser with a Cu-Kα source radiation, step intervals of 0.02°, and 30 kV and 10 mA as the voltage and current conditions, respectively.

2.3. Porosity and density measurements

The porosity and density of the sintering samples were estimated by the Archimedes method according to ASTM B962-17. The Archimedes method has proven to be extremely accurate, with a standard deviation value of ±<0.1% [23]. The average porosity was obtained from at least five measurements on each sample. Alloys were precision-weighed on a KERN 770 balance (0.0001 g accuracy). Pore diameter and morphology were analyzed by optical microscopy.

2.4. Mechanical characterization

In order to evaluate the mechanical properties of the Ti–2.5In, Ti–5In, and Ti–10In alloys, samples' elastic modulus was obtained by the nondestructive impulse excitation technique (IET) with Sonelastic equipment. At least four measurements were taken on five different samples for each Ti/In weight ratio. To obtain the bending strength of each alloy, three-point tests were run on a Shimadzu Autograph AG-100 KN Xplus universal testing machine. Bending tests were performed according to ISO 3325/A1:2002 at a constant deformation speed of 0.5 mm/min and a 22 mm distance between supports. To estimate bending strengths, the equation $\sigma = 3PL/2bh^2$ was used, where σ is bending strength (MPa), P is load (N), L is span length (mm), b is specimen width (mm) and h is specimen thickness (mm). To obtain good estimations, five samples of every Ti/In ratio were tested. A Centaur durometer model HD9-45 was used to take the Rockwell superficial hardness measurements (HR15N). Samples were tested by applying 147 N for 10 s with the previous surface grinding preparation. At least 20 measurements were obtained per alloy.

2.5. Ion release tests

For the ion release study, three samples of each alloy were immersed in 50 mL of artificial saliva at a concentration of hydrogen ions (pH) of 5.270 ± 0.108 (see Table 1 for composition details) and were incubated for 730 h at 37 °C. After incubation, the morphology of samples was studied under OM and SEM. Inductively coupled plasma optical emission spectrometry (ICP-OES) was performed using Varian-715ES equipment to measure the concentrations of Ti^{3+} and In^{3+} ions dissolved in the incubated medium.

2.6. Corrosion behavior study

The evaluation corrosion resistance was carried out for two samples of each alloy by a PGSTAT204 potentiostat (Metrohm AUTOLAB). A reference Ag/AgCl electrode, a platinum counter electrode, and Fusayama artificial saliva with a pH of 5.030 ± 0.003 at 37 °C as an electrolyte were used in the electrochemical cell. Table 1 shows the chemical composition of the Fusayama artificial saliva. Measurements were taken using a sinusoidal perturbation of 10 mV amplitude and a frequency range from 10^4 to 10^{-3} Hz. The data analysis was performed by the Nova 2.1.1 software.

3. Results and discussion

3.1. Microstructural evaluation

The three fabricated alloys, Ti–2.5In, Ti–5In, and Ti–10In, were single-phase. Fig. 1a shows the XRD measurements of the three obtained alloys, where it is possible to identify the main peaks related to the alpha hexagonal phase. As indicated in Fig. 1b, XRD results agreed with that expected for In contents up to 20 wt.%, i. e., a monophasic microstructure in the alpha region [21,22]. Fig. 2a–2c obtained by OM depict the morphology and size of the alpha phase grains, and how grain size reduced according to In content. While the Ti–2.5In alloy presented grains within the 80–450 μm range, grains were small for Ti–10In (10–40 μm). This grain size reduction was 11.2-fold when comparing the 2.5 and 10 wt.% In conditions. The effect of In on the refinement and equiaxiality of grains has been reported for other metallic alloys [24]. To understand the origin of decreasing grain size with the In content it is necessary to study deeply the atomic diffusion process into the microstructures. Fig. 2d–2i let reveal the presence of porosity in the Ti–In alloys as a result of the powder metallurgical process. Porosity was homogeneously dispersed in the alloy with a semi-equiaxial morphology and rounded pore edges. The pore morphology did not show any apparent variation when increasing In. Pore size with diameters ranging from 5 to 25 μm did not show any noticeable changes among the three manufactured alloys.

For further study of the diffusion process into the alloys, EDS analyses shown in Fig. 3a–c depict the linear distribution of Ti and In across two interceptions of a grain boundary. Here we can see the higher In content on the boundaries compared to grains. This phenomenon could be a joint effect with the In segregation on the grain boundaries, which are extensively reported as high-energy and metastable zones that lead to segregation and nucleation phenomena [25]. In Fig. 3e and f a

Table 1 – Chemical composition of artificial saliva for the ion release study (pH 5.2) and the Fusayama artificial saliva for corrosion tests.

Chemical compound	Concentration/g L^{-1}	
	Ions release	Electrochemical test
NaCl	0.4	0.4
$CaCl_2$	0.8	0.625
Urea	1	1
$Na_2S \cdot 3H_2O$	0.004	0.0044
$NaH_2PO_4 \cdot H_2O$	0.53	0.531
KCl	0.4	0.4
NaF	2.5	-
Distilled water	Up to 1 L	Up to 1 L

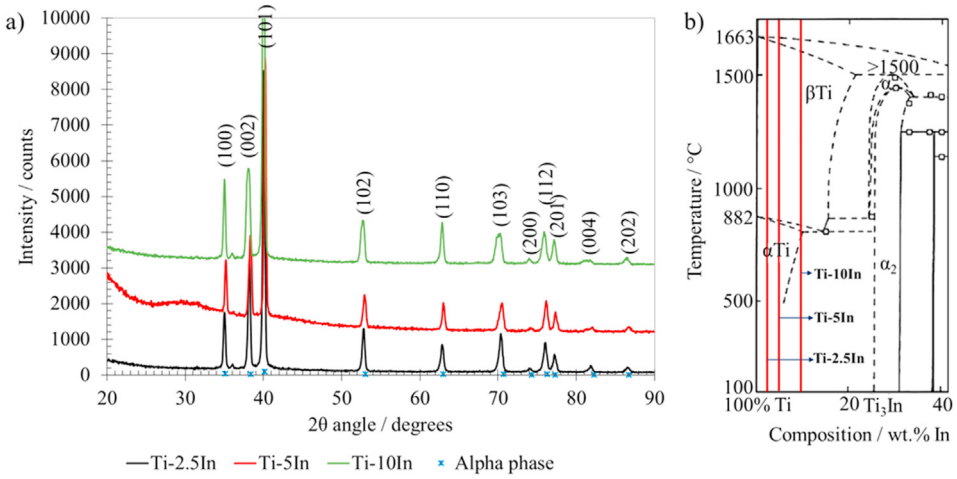

Fig. 1 – a) XRD patterns of Ti–2.5In, Ti–5In, and Ti–10In alloys and b) relevant region of the Ti–In phase diagram, adapted from [22].

larger statistic of grain frontiers and porous regions rich in In can be seen, while Ti content is mainly present within the grain. The heterogeneous infiltration of In within the grains could be improved by elevating the temperature of the sintering process. However, it would also cause the decline of the mechanical properties of the alloy [26]. The reduced atomic mobility with the In content may be the reason for the grain refinement showed in Fig. 2. This is, In may be acting as an anchor for the diffusion of Ti throughout the grains, slowing grain growth during the sintering process. The effect of low-diffused particles as a pin in the grain boundary to stop the growth is known [27]. A similar effect of In as grain refiner on the microstructure of gold films has been already reported [24].

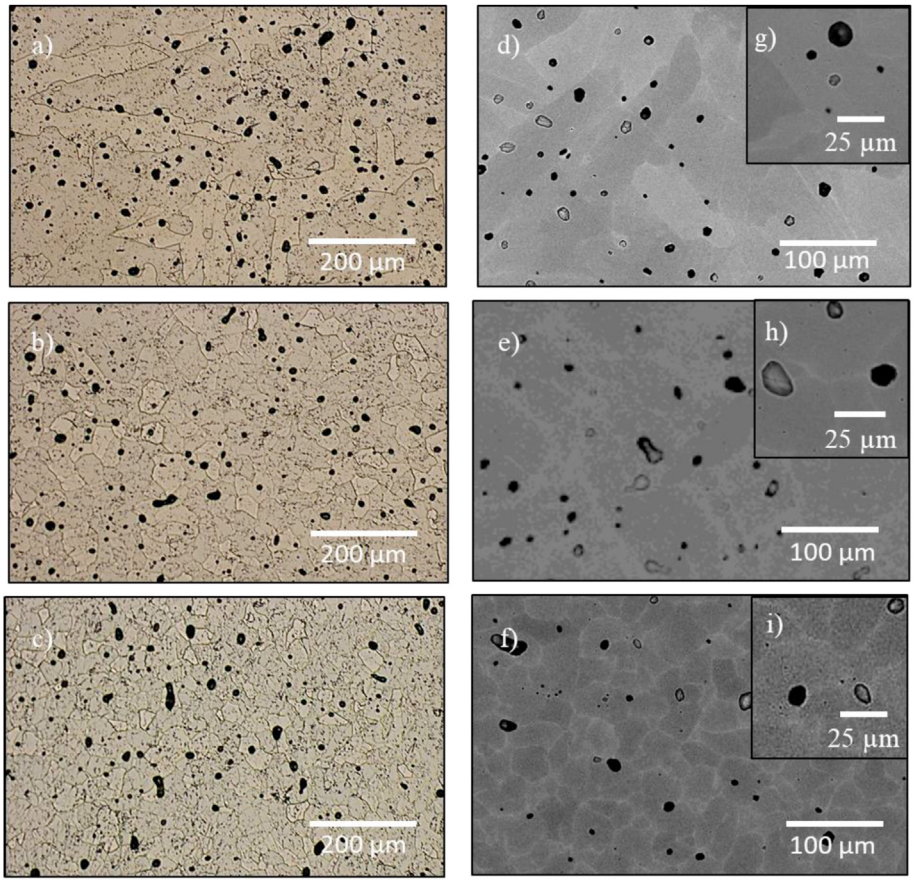

Fig. 2 – Single-phase microstructure and porosity conditions by OM and SEM, respectively of a, d, g) Ti–2.5In, b, e, h) Ti–5In, and c, f, i) Ti–10In alloys.

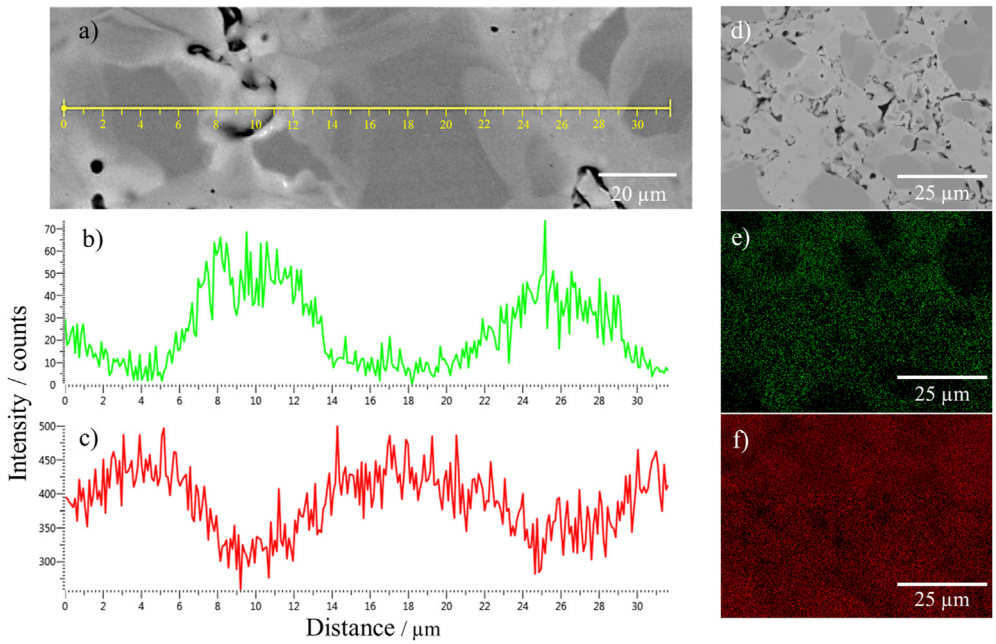

Fig. 3 – Ti and In distribution in Ti–0In alloys by EDS, a-c) linear analysis and d-f) mapping, where a, d) micrographs, b, e) In content, and c, f) Ti content.

3.2. *Porosity and density measurements*

By considering the absolute In density, which is approximately 62% higher than that of Ti, the relative density of the manufactured Ti–In alloys should increase with In content. This increase in relative density is seen in Fig. 4. The decreased closed porosity and the increment in open porosity according to In content are also observed. The inverse relationship between open and closed porosities as In content increases is the result of the lower melting point of In (156.6 °C). As it cools, the infiltration of the molten low-melting-point metal into the adjacent volume fills a part of the pores, reducing the closed porosity of the solid body. Fig. 3 supports the premise of In infiltration on grain boundaries and pores with a low diffusion within the grain. Infiltration of low-melting-point metals during sintering is a widely reported phenomenon [28]. The increasing open porosity tendency could be due to the bigger In sublimation volume as a result of the higher In content in the alloy. The increased volume of the gaseous metal moving toward the surface could end in the porosity adjacent to the surface. It is worthy to mention that increasing open porosity in the microstructure may be beneficial by providing local environments for bone formation [29].

3.3. *Mechanical characterization*

To compare the porosity and mechanical behaviors of the Ti–2.5In, Ti–5In, and Ti–10In alloys, Fig. 5 shows the hardness, bending strength, and elastic modulus graphs according to In content. An elastic modulus ranging from 114.6 to 116.5 GPa led to slight changes appearing among the three fabricated Ti–In alloys, but no clear relation to In content or porosity appeared. The modulus of Ti–10In, 116.6 GPa, was

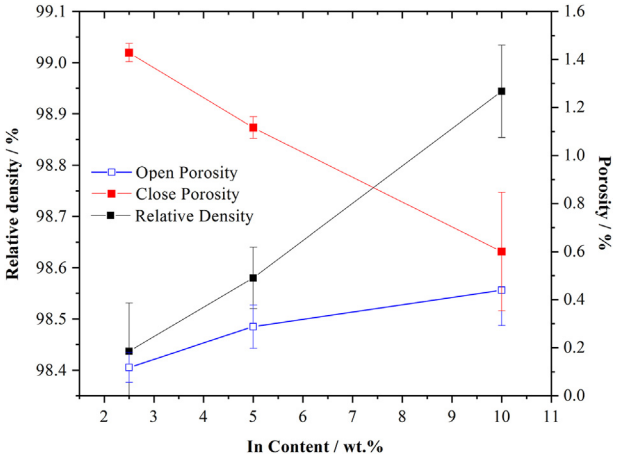

Fig. 4 – Relative density, close and open porosity according to In content.

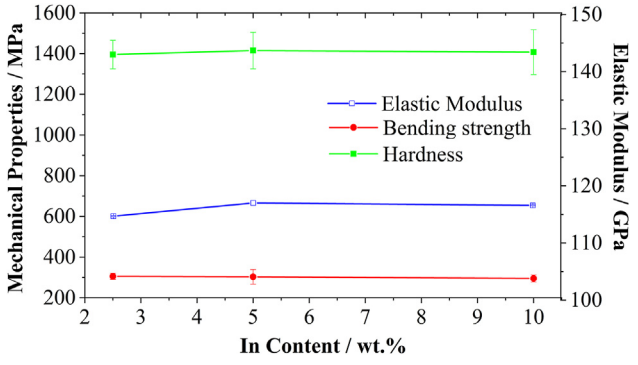

Fig. 5 – Mechanical properties of the Ti–In alloys according to In content.

Table 2 – Comparison of mechanical properties and porosity of the studied Ti–In alloys and CP–Ti.

Alloy	E, GPa	σ, MPa	Hardness, MPa	Poisson coefficient	Total porosity, %
Ti–2.5In	114.7 ± 0.1	319.4 ± 15	1395 ± 70	0.38	1.5 ± 0.1
Ti–5In	117.0 ± 0.0	317.1 ± 36	1415 ± 90	0.37	1.4 ± 0.1
Ti–10In	116.5 ± 0.1	309.0 ± 17	1407 ± 110	0.38	1 ± 0.05
CP–Ti	102.7[a]	680–770[b]	1324–2059[c]	0.34[a]	5.1[b]

[a] Annealed CP-Ti (grade 1) [36].
[b] Porous CP-Ti (grade 2) prepared by powder sintering technique [37].
[c] Porous CP-Ti (grade 4) obtained by sintering and pressing process [31].

slightly below the value for the same composition alloy under the cast condition of 124.1 GPa [21]. This dropped of the modulus of Ti–10In alloy is congruent with the reported decrement of the elastic modulus with the addition of In to Ti-based alloys [30]. Both hardness and bending strength remained almost constant with the variation of In content and did not show any direct dependence on grain size. This could be related to the simultaneous action of two mechanisms; 1) strengthening due to grain refinement; 2) softening at grain boundaries and in porous regions due to heterogeneous In distribution. This phenomenon may not be abnormal for powder metallurgy materials, as they do not always comply with the classic inverse relation between mechanical strength and hardness with the grain size of alloys. Explaining such an effect can be associated with the combined effects of relative density, pore morphology, gas content, chemical heterogeneities, among other structural defects. Such non-classic behavior has been reported for elemental Ti by pressing and sintering techniques in which hardness increased with grain growth [31]. The bending strength of all the Ti–In samples, with values around 0.3 GPa, came close to that of human bone, reported lying between 0.35 and 0.39 GPa [32]. In addition, total porosity decreased with In addition, which is consistent with the increased relative density shown in Fig. 4. The importance of porosity in the performance of dental implants is highlighted because, as formerly reported, the presence of pores can favor a lower elastic modulus [19,33]. Furthermore, the porous region can act as a "titanium/bone composite" to compensate the mismatch of the elastic modulus between them [16]. For a deeper understanding of the effect of porosity in the Ti–In alloys, Eq. (1) provides guidelines for estimating the elastic modulus of porous materials [34]:

$$E = E_0(1-2\varphi)\left(1+4\varphi^2\right) \quad (1)$$

where E is the theoretical Young's modulus, E_0 is the elastic modulus when porosity is zero and φ is the porosity. Considering the total porosity values for Ti–5In and Ti–10In alloys (Table 2) and the values of E for the same alloys obtained by arc-melting [21], Eq. (1) was applied. This empiric equation was developed for materials less than 30% of porosity and Poisson coefficient near 0.3. This equation also includes some limitations, such as no consideration of microstructure defects and condition, as well as the thermo-mechanic history of the porous materials. From the literature, the E_0 for Ti–5In and Ti–10In are 159.8 and 124.1 GPa, respectively. Substituting previous values on Eq (1), elastic moduli of 155.3 and 121.5 GPa are obtained for Ti–5In and Ti–10In alloys, respectively.

Comparing the theoretical approximations with the experimental data from Table 2, it is possible to highlight two important events: experimental values are down to the expectations and the Ti–5In alloy presents values farther from it. The Ti–10In alloy is 4% down to the theoretical calculation, while the Ti–5In is lower by 24.7%. Both events might be related to the grain size differences and the low In diffusion into the Ti-matrix which were showed in Figs. 2 and 3. The Ti–5In alloy has a greater grain size and less quantity of the heterogeneous distributed In into the microstructure, while the strengthening of Ti–10In is potentiated by the lower grain sizes. The combination of these effects may trigger the deformation out of the theoretical limits in a more evident way for Ti–5In in comparison with Ti–10In. From the use of Eq (1) it is also possible to note the bigger effect of grain size and In content on the mechanical behavior than the effect of porosity, probably because of the low porosity percentage. Table 2 compares the mechanical properties and porosity of the studied Ti–In alloys and commercially pure Ti (CP–Ti) from literature. The obtained hardness values, which went from 1.39 to 1.41 GPa, fell within the range of the elemental Ti; i.e., between 1.3 and 2.0 GPa [31]. Alloys with hardness less than 1.22 GPa are generally susceptible to wear damage, while alloys harder than 3.33 GPa may promote wearing on opposite teeth [35]. Elastic modulus and bending strength were lower for Ti–In alloys in comparison with the reported for CP-Ti. Such behavior might be explained in terms of the heterogeneous distribution of In on the microstructure.

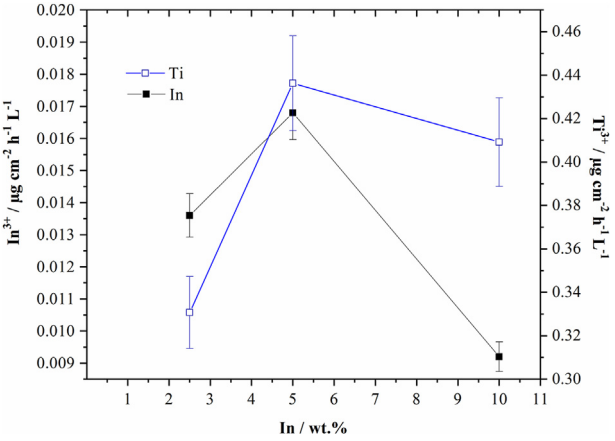

Fig. 6 – Concentration of the released In^{3+} and Ti^{3+} ions according to In content.

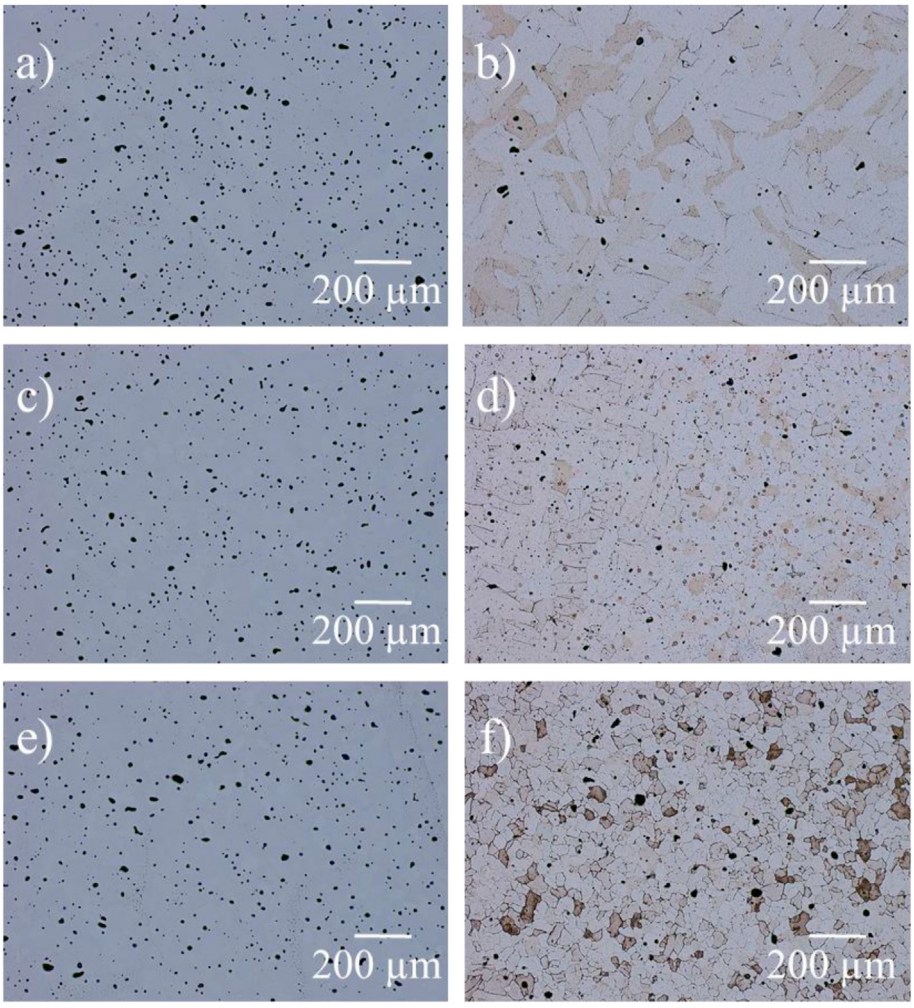

Fig. 7 – OM micrographs of alloys a, b) Ti–2.5In, c, d) Ti–5In and e, f) Ti–10In when comparing conditions a, c, e) before and b, d, f) after the ion release test.

3.4. *Ion release tests*

Assessing ion release levels is extremely important for biomaterials because released elements can play a role in health after diffusing into the body. The concentrations of the Ti and In ions released from the Ti–2.5In, Ti–5In, and Ti–10In alloys in artificial saliva are shown in Fig. 6. No clear tendency of the released Ti^{3+} and In^{3+} ion according to In content was observed. However, both graphs indicate increasing values or the released ions in samples Ti–5In, 0.436 and 0.017 μg cm^{-2} h^{-1} L^{-1} for Ti and In, respectively, compared to the Ti–2.5In alloy, where the concentrations of Ti^{3+} and In^{3+} were 0.331 and 0.014 μg cm^{-2} h^{-1} L^{-1}, respectively. However, both graphs show lowering concentration values of the Ti–10In sample, where 0.4092 and 0.0092 μg cm^{-2} h^{-1} L^{-1} were obtained for Ti^{3+} and In^{3+}, respectively. This drop could be related to the incremented relative density. It is noteworthy that the Ti^{3+} concentrations of the three alloys were well below the limit of 10 ppm (10000 μg L^{-1}), which has been reported as an inhibitor of cell proliferation [38]. However, the obtained ion release concentrations of Ti^{3+} ranging from 0.3 to 0.4 μg cm^{-2} h^{-1} L^{-1} are higher than those reported for CP-Ti (grade 2). These values range from 0.2 to 0.3 μg cm^{-2} h^{-1} L^{-1} for 504 and 1008 immersion hours, respectively [39]. All the concentrations of the In ions were well below 2310 μM ($2.65 \cdot 10^5$ μg L^{-1}), which is the limit concentration that causes 50% cell death (TC50) for L-929 fibroblasts [40].

As the main reason for metal ion release from dental implants is a result of the corrosion process triggered by the interaction between the implanted material and oral fluids

Table 3 – Parameters of the equivalent circuit.

Sample	R_s, Ω cm^2	CPE_{dl}, μF cm^2	R_c, Ω cm^2	CPE_{pc}, μF cm^2	R_{pc}, Ω cm^2	χ^2
Ti–2.5In	1.68E-05	7.90E-07	9.98E+01	3.02E-05	6.37E+06	1.50E-03
Ti–5In	1.63E-04	1.27E-08	1.22E+02	3.10E-05	4.37E+06	1.19E-03
Ti–10In	8.52E-05	1.41E-06	1.15E+02	2.82E-05	2.67E+06	1.11E-03

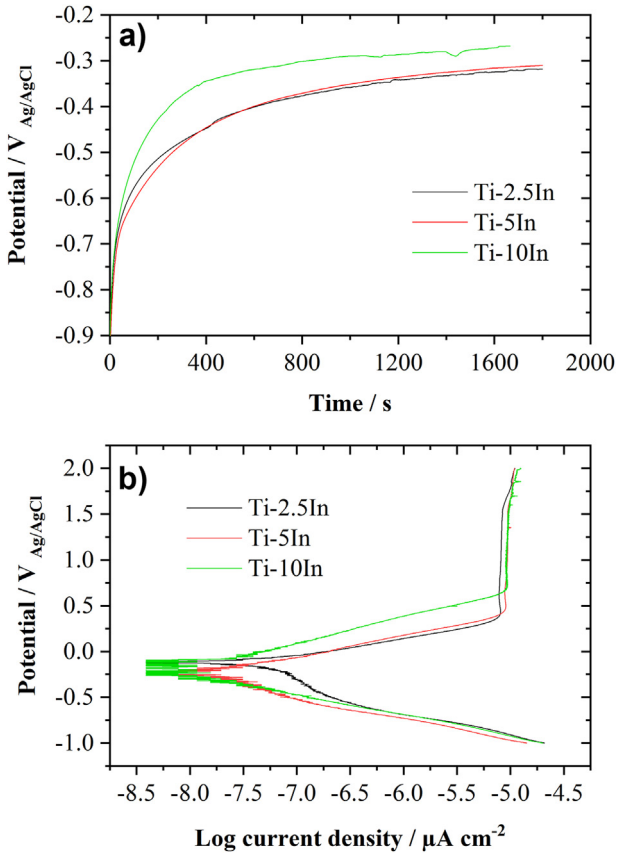

Fig. 8 – a) Open circuit potential (OCP) and b) potentiodynamic (PD) curves of alloys Ti–2.5In, Ti–5In, and Ti–10In.

[41], it is important to discern the microstructural changes generated by the corrosive medium of artificial saliva. Fig. 7 offers the OM micrographs obtained with Ti–2.5In, Ti–5In, and Ti–10In before and after being subjected to corrosive medium. The effect of artificial saliva is evident in all the samples as it delimited the grain boundaries, as well as revealed the grains with higher In content as the lighter areas. This is congruent with the heterogeneous diffusion of In on the Ti matrix, which was explained previously in Fig. 3. Likewise, in Fig. 7f, which corresponds to alloy Ti–10In, it was the most attacked by the medium. As it can be seen in Fig. 7, no evident cracks or localized corrosion were produced by the corrosive environment in any of the three tested samples.

3.5. *Corrosion behavior study*

Fig. 8a presents the open circuit potential (OCP) graphs of the Ti–In alloys, along with immersion in artificial Fusayama saliva. The OCP is assumed to indicate the surface transition of alloys from passive to active. The corrosion potential increased in the primary immersion stage and then remained almost constant from the 400 s immersion time. We can see that alloys stabilized with less negative potentials according to the In wt.% content. It can be seen a rise of potential for the Ti–10In, which can be an indicator of lower degradation probability [42]. The OCP values stabilized quickly enough, which indicates efficient passive oxide layer formation. This observation was corroborated by the potentiodynamic (PD) curves (Fig. 8b) of the Ti–2.5In, Ti–5In, and Ti–10In alloys in artificial Fusayama saliva solution. The Ti–5In and Ti–10In alloys showed similar polarization behavior. After cathodic polarization, all the samples revealed superficial passivation, as indicated by the constant current densities with

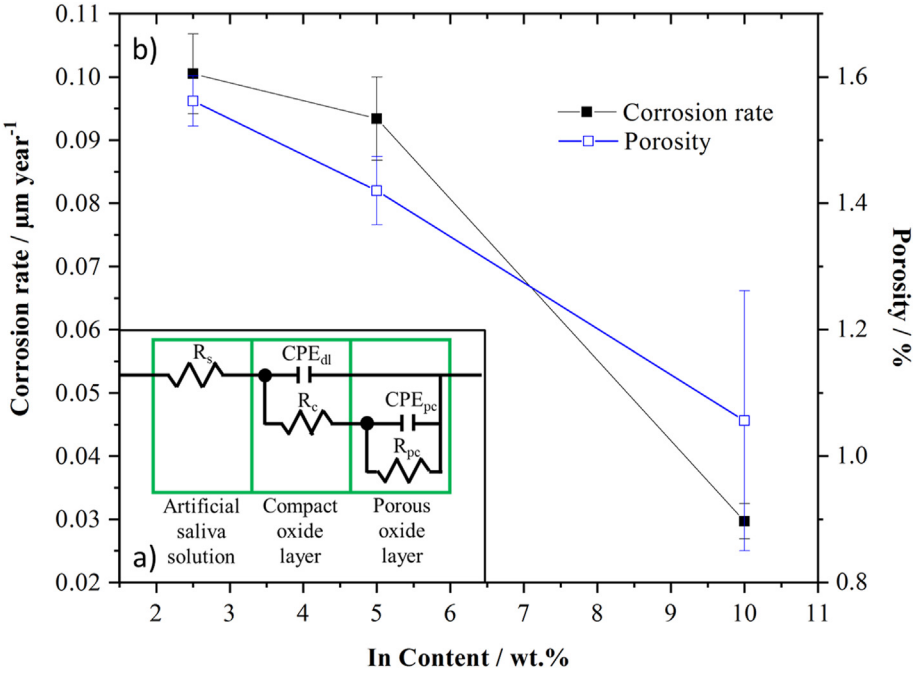

Fig. 9 – a) Equivalent circuit of the electrochemical system used in this work and b) the corrosion rate and total porosity according to In content.

incremented potential. The relevance of this passive layer lies in protecting the material surface from corrosion, which occurs when the oxide film is damaged by coming into contact with other oral environment components [39]. The passivation current densities of the three Ti–In alloys were similar, at around 10^{-5} μA cm^{-2} at 2 V, which suggests comparable corrosion resistance behavior.

Fig. 9a displays the equivalent circuit used to investigate the corrosion mechanism. The setting values are summarized in Table 3, including the χ^2 value, which is widely used as an indicator of the expected values to compare the experimental data. The equivalent circuit was constituted by the electrolyte, a compact oxide layer that blocks the electrolyte from passing, and a porous oxide layer that confers more stability against the penetration of the ions that resulted from the corrosion process. The presence of oxides to create a passive TiO_2 layer is essential for protecting the alloy from the external diffusion of metal ions [43,44]. In this circuit, R_s, R_c, and R_{pc} were the solution resistances between the working electrode and the reference electrode, the resistance between both oxide layers, and the resistance between the porous layer and the alloy, respectively. In more detail: (i) the R_c element was related to the high-frequency contribution and was parallel to a double layer capacitance; (ii) CPE_{dl} was related to the dielectric properties of the compact oxide layer; (iii) R_{pc} was related to the low-frequency contribution and paralleled a constant phase element; and (iv) CPE_{pc} represents charge transfer resistance. Figure 9b compares the trends of the corrosion rate and the total porosity of each alloy according to In content. Both graphs follow the same downward trend with In increment. This sensitivity of corrosion with In content is a consistent phenomenon that has been reported for other Ti–In alloys obtained by arc melting [21]. It is worthy to point the drop of ion release and corrosion rate values from Figs. 6 and 9, as well as the higher OCP value from Fig. 8a. Those tendencies may indicate a protective effect of the In to the Ti-matrix, which is more evident for the Ti–10In sample. It has been reported the formation of a passivation layer triggered by the addition of In in Al- and Ti-based alloys [45–47]. Likewise, the formation of the surface oxide film was indicated by the constant current densities after cathodic polarization from Fig. 8b. The indium oxides have been also reported as a bonding agent in metallic biomaterials surfaces [20,48].

4. Conclusions

The three fabricated Ti–2.5In, Ti–5In, and Ti–10In alloys clearly showed the role of In addition as a grain refiner. The low-diffused In particles into the Ti-matrix acted as a pin in the grain boundary to stop the growth. This phenomenon led to a reduction in grain size from a maximum of 450 to 40 μm for the Ti–2.5In and Ti–10In samples, respectively. This is an 11.2-fold grain size reduction. The total porosity of the Ti–In alloys decreased according to In content. However, grain size and In content showed a greater effect on the mechanical behavior in comparison with the effect of porosity, probably because of the low porosity percentage. Furthermore, the three prepared Ti–In alloys showed non-classic mechanical performance as strength and hardness did not correspond to the expected response according to the obtained grain refinement. This phenomenon can be attributed to the heterogeneous In distribution, predominantly on the grain boundaries and porous regions. The bending strength and hardness values were between the acceptable ranges for resisting permanent deformation and adequate wear resistance with no risky opposition to teeth. The Ti^{3+} and In^{3+} ion releases were below the toxic concentrations, which proves that the Ti–In alloys prepared by powder metallurgy methods are feasible candidates for dental prosthesis. Corrosion behavior was dominated by efficient oxide passive layer formation, which led to corrosion rates between 0.02 and 0.1 μm $year^{-1}$. The corrosion rate lowered with In addition. The drop of ion release and corrosion rate values with the In content, as well as the higher OCP value, indicate a protective effect of the indium to the Ti-matrix, which is more evident for the Ti–10In sample. Given the set of the smaller grain sizes, the highest open porosity percentage, the lower values of the Ti^{3+} and In^{3+} ion releases, and the lower corrosion rate, it is possible to predict from the three sintered alloys that the Ti–10In alloy could offer the most appropriate dental implant performance.

Funding

This work was supported by the Ministerio Español de Ciencia, Innovación y Universidades, Spain with Grant RTI2018-097810-B-I00, and the European Union (EU) through Fondo Europeo de Desarrollo Regional (FEDER), Spain.

Data availability

The raw data related to this manuscript would be made available on request.

Declaration of Competing Interest

The authors declare that they have no known competing financial interests or personal relationships that could have appeared to influence the work reported in this paper.

Acknowledgments

The authors would like to thank the valuable technical support provided by J. C. Zambrano Carrullo.

REFERENCES

[1] Gaviria L, Salcido JP, Guda T, Ong JL. Current trends in dental implants. J Korean Assoc Oral Maxillofac Surg 2014;40:50. https://doi.org/10.5125/jkaoms.2014.40.2.50.

[2] Alrabeah GO, Brett P, Knowles JC, Petridis H. The effect of metal ions released from different dental implant-abutment couples on osteoblast function and secretion of bone

resorbing mediators. J Dent 2017;66:91–101. https://doi.org/10.1016/j.jdent.2017.08.002.
[3] Messer R, Wataha J. Dental Materials: biocompatibility. Encycl Mater Sci Technol 2002:1–10.
[4] Okabe T, Hero H. The use of titanium in dentistry. Cells Mater 1995;5:211–30.
[5] Prasad S, Ehrensberger M, Gibson MP, Kim H, Monaco EA. Biomaterial properties of titanium in dentistry. J Oral Biosci 2015;57:192–9. https://doi.org/10.1016/j.job.2015.08.001.
[6] Gosavi S, Gosavi S, Alla R. Titanium: a miracle metal in dentistry. Trends Biomater Artif Organs 2013;27:42–6.
[7] Li JP, Li SH, Van Blitterswijk CA, De Groot K. A novel porous Ti6A14V: characterization and cell attachment. J Biomed Mater Res 2005;73:223–33. https://doi.org/10.1002/jbm.a.30278.
[8] Lee BH, Kim Y Do, Lee KH. XPS study of bioactive graded layer in Ti-In-Nb-Ta alloy prepared by alkali and heat treatments. Biomaterials 2003;24:2257–66. https://doi.org/10.1016/S0142-9612(03)00034-6.
[9] Faria ACL, Rodrigues RCS, Rosa AL, Ribeiro RF. Experimental titanium alloys for dental applications. J Prosthet Dent 2014;112:1448–60. https://doi.org/10.1016/j.prosdent.2013.12.025.
[10] Bomfim PK dos S, Ciuccio R, Neves MDM das. Development of titanium dental implants using techniques of powder metallurgy. Mater Sci Forum 2014;775–776:13–8. https://doi.org/10.4028/www.scientific.net/MSF.775-776.13.
[11] Espevik S, Oilo G, Lodding A. Oxidation of noble metal alloys for porcelain veneer crowns. Acta Odontol Scand 1979;37:323–8. https://doi.org/10.3109/00016357909004703.
[12] Gebert A, Oswald S, Helth A, Voss A, Flaviu P, Rohnke M, et al. Effect of indium (In) on corrosion and passivity of a beta-type Ti – Nb alloy in Ringer's solution. Appl Surf Sci 2015;335:213–22. https://doi.org/10.1016/j.apsusc.2015.02.058.
[13] Hornez JC, Lefèvre A, Joly D, Hildebrand HF. Multiple parameter cytotoxicity index on dental alloys and pure metals. Biomol Eng 2002;19:103–17. https://doi.org/10.1016/S1389-0344(02)00017-5.
[14] Banerjee D, Williams JC. Perspectives on titanium science and technology. Acta Mater 2013;61:844–79. https://doi.org/10.1016/j.actamat.2012.10.043.
[15] Murray GAW, Semple JC. Transfer of tensile loads from a prosthesis to bone using porous titanium. J Bone Jt Surg 1981;63B:138–41. https://doi.org/10.1302/0301-620X.63B1.7204467.
[16] Vasconcellos LMR de, Carvalho YR, do Prado RF, Vasconcellos LGO de, Graca ML de A, Cairo CAA. Porous titanium by powder metallurgy for biomedical application: characterization , cell citotoxity and in vivo tests of osseointegration. Biomed Eng Tech Appl Med 2012:48–74. https://doi.org/https://doi.org/10.5772/47816.
[17] Bram M, Ebel T, Wolff M, Barbosa APC, Tuncer N. Applications of powder metallurgy in biomaterials. Adv Powder Metall 2013:520–54. https://doi.org/10.1533/9780857098900.4.520.
[18] Goia TS, Violin KB, Yoshimoto M, Bressiani JC, Bressiani AHA. Osseointegration of titanium alloy macroporous implants obtained by PM with addition of gelatin. Adv Sci Technol 2010;76:259–63. https://doi.org/10.4028/www.scientific.net/ast.76.259.
[19] Xu W, Liu Z, Lu X, Tian J, Chen G, Liu B, et al. Porous Ti-10Mo alloy fabricated by powder metallurgy for promoting bone regeneration. Sci China Mater 2019;62:1053–64. https://doi.org/10.1007/s40843-018-9394-9.
[20] Wang QY, Wang YB, Lin JP, Zheng YF. Development and properties of Ti – in binary alloys as dental biomaterials. Mater Sci Eng C 2013;33:1601–6. https://doi.org/10.1016/j.msec.2012.12.070.
[21] Han MK, Im JB, Hwang MJ, Kim BJ, Kim HY, Park YJ. Effect of indium content on the microstructure, mechanical properties and corrosion behavior of titanium alloys. Metals 2015;5:850–62. https://doi.org/10.3390/met5020850.
[22] Gulay LD, Schuster JC. Investigation of the titanium–indium system. J Alloys Compd 2003;360:137–42. https://doi.org/doi:10.1016/S0925-8388(03)00319-0.
[23] Spierings AB, Schneider M, Eggenberger R. Comparison of density measurement techniques for additive manufactured metallic parts. Rapid Prototyp J 2011;17:380–6. https://doi.org/10.1108/13552541111156504.
[24] Lee SY, Hummel RE, Dehoff RT. On the role of indium underlays in the prevention of thermal grooving in thin gold films. Thin Solid Films 1987;149:29–48. https://doi.org/10.1016/0040-6090(87)90246-X.
[25] Li L, Kamachali RD, Li Z, Zhang Z. Grain boundary energy effect on grain boundary segregation in an equiatomic high-entropy alloy. Phys Rev Mater 2020;4:53603. https://doi.org/10.1103/PhysRevMaterials.4.053603.
[26] Chen X, Ni D, Kan Y, Jiang Y, Zhou H, Wang Z, et al. Reaction mechanism and microstructure development of ZrSi2 melt-infiltrated Cf/SiC-ZrC-ZrB2 composites: the influence of preform pore structures. J Mater 2018;4:266–75. https://doi.org/10.1016/j.jmat.2018.05.005.
[27] Ahmed K, Tonks M, Zhang Y, Biner B, El-Azab A. Particle-grain boundary interactions: a phase field study. Comput Mater Sci 2017;134:25–37. https://doi.org/10.1016/j.commatsci.2017.03.025.
[28] Kazuo Y, Gongli Y. Method for forming titanium alloys by powder metallurgy. 1999. 5,930,583.
[29] Simmons CA, Meguid SA, Pilliar RM. Differences in osseointegration rate due to implant surface geometry can be explained by local tissue strains. J Orthop Res 2001;19:187–94. https://doi.org/10.1016/S0736-0266(00)90006-8.
[30] Calin M, Helth A, Gutierrez Moreno JJ, Bönisch M, Brackmann V, Giebeler L, et al. Elastic softening of β-type Ti-Nb alloys by indium (In) additions. J Mech Behav Biomed Mater 2014;39:162–74. https://doi.org/10.1016/j.jmbbm.2014.07.010.
[31] Bolzoni L, Ruiz-Navas EM, Gordo E. Processing of elemental titanium by powder metallurgy techniques. Mater Sci Forum 2013;765:383–7. https://doi.org/10.4028/www.scientific.net/MSF.765.383.
[32] Rho JY, Kuhn-Spearing L, Zioupos P. Mechanical properties and the hierarchical structure of bone. Med Eng Phys 1998;20:92–102. https://doi.org/10.1016/S1350-4533(98)00007-1.
[33] Nune KC, Li S, Misra RDK. Advancements in three-dimensional titanium alloy mesh scaffolds fabricated by electron beam melting for biomedical devices: mechanical and biological aspects. Sci China Mater 2018;61:455–74. https://doi.org/10.1007/s40843-017-9134-x.
[34] Lu G, Lu GQ, Xiao ZM. Mechanical properties of porous materials. J Porous Mater 1999;6:359–68. https://doi.org/10.1023/a:1009669730778.
[35] Wataha JC. Alloys for prosthodontic restorations. J Prosthet Dent 2002;87:351–63. https://doi.org/10.1067/mpr.2002.123817.
[36] Bieler TR, Trevino RM, Zeng L. Alloys: titanium. Encycl Condens Matter Phys 2005:65–76. https://doi.org/10.1016/B0-12-369401-9/00536-2.
[37] Oh IH, Nomura N, Masahashi N, Hanada S. Mechanical properties of porous titanium compacts prepared by powder

sintering. Scripta Mater 2003;49:1197–202. https://doi.org/10.1016/j.scriptamat.2003.08.018.

[38] Liao H, Wurtz T, Li J. Influence of titanium ion on mineral formation and properties of osteoid nodules in rat calvaria cultures. J Biomed Mater Res 1999;47:220–7. https://doi.org/10.1002/(SICI)1097-4636(199911)47:2<220::AID-JBM12>3.0.CO;2-9.

[39] Dimć ID, Cvijović-Alagić IL, Rakin MB, Perić-Grujić AA, Rakin MP, Bugarski BM, et al. Effect of the pH of artificial saliva on ion release from commercially pure titanium. Acta Period Technol 2013;44:207–15. https://doi.org/10.2298/APT1344207D.

[40] Schmalz G, Arenholt-Bindslev D, Pfüller S, Schweikl H. Cytotoxicity of metal cations used in dental cast alloys. ATLA Altern to Lab Anim 1997;25:323–30. https://doi.org/10.1177/026119299702500313.

[41] Dimic I, Cvijovic-Alagic I, Rakin M, Branko B. Analysis of metal ion release from biomedical. Mater Eng 2013;19(2):167–76.

[42] Ferrel-álvarez AC, Domínguez-Crespo MA, Torres-Huerta AM, Cong H, Brachetti-Sibaja SB, López-Oyama AB. Intensification of electrochemical performance of AA7075 aluminum alloys using rare earth functionalized water-based polymer coatings. Polymers 2017;9:178. https://doi.org/10.3390/polym9050178.

[43] Huang HH, Chiu YH, Lee TH, Wu SC, Yang HW, Su KH, et al. Ion release from NiTi orthodontic wires in artificial saliva with various acidities. Biomaterials 2003;24:3585–92. https://doi.org/10.1016/S0142-9612(03)00188-1.

[44] Zhang BB, Zheng YF, Liu Y. Effect of Ag on the corrosion behavior of Ti-Ag alloys in artificial saliva solutions. Dent Mater 2009;25:672–7. https://doi.org/10.1016/j.dental.2008.10.016.

[45] Pilz S, Gebert A, Voss A, Oswald S, Göttlicher M, Hempel U, et al. Metal release and cell biological compatibility of beta-type Ti-40Nb containing indium. J Biomed Mater Res B Appl Biomater 2018;106:1686–97. https://doi.org/10.1002/jbm.b.33976.

[46] Wu Z, Zhang H, Qin K, Zou J, Qin K, Ban C, et al. The role of gallium and indium in improving the electrochemical characteristics of Al–Mg–Sn-based alloy for Al–air battery anodes in 2 M NaCl solution. J Mater Sci 2020;55:11545–60. https://doi.org/10.1007/s10853-020-04755-8.

[47] Gudić S, Smoljko I, Klikić M. The effect of small addition of tin and indium on the corrosion behavior of aluminium in chloride solution. J Alloys Compd 2010;505:54–63. https://doi.org/10.1016/j.jallcom.2010.06.055.

[48] Morris HF, Manz M, Stoffer W, Weir D. Casting alloys: the materials and “the clinical effects.”. Adv Dent Res 1992;6:28–31. https://doi.org/10.1177/08959374920060011101.